Nonlinear Tracking Control with Reduced Complexity of Serial Robots: A Robust Fuzzy Descriptor Approach

Thi van Anh Nguyen, Tran Anh-Tu Nguyen, Antoine Dequidt, Laurent Vermeiren, Michel Dambrine

Nonlinear Tracking Control with Reduced Complexity of Serial Robots: A Robust Fuzzy Descriptor Approach

Article *in* International Journal of Fuzzy Systems · March 2019

DOI: 10.1007/s40815-019-00613-1

CITATIONS
15

READS
596

5 authors, including:

Anh-Tu Nguyen
Université Polytechnique Hauts-de-France
140 PUBLICATIONS **2,084** CITATIONS
SEE PROFILE

Antoine Dequidt
Université Polytechnique Hauts-de-France
77 PUBLICATIONS **470** CITATIONS
SEE PROFILE

Laurent Vermeiren
Université Polytechnique Hauts-de-France
82 PUBLICATIONS **1,776** CITATIONS
SEE PROFILE

Michel Dambrine
Université Polytechnique Hauts-de-France
151 PUBLICATIONS **4,316** CITATIONS
SEE PROFILE

Noname manuscript No.
(will be inserted by the editor)

Nonlinear Tracking Control with Reduced Complexity of Serial Robots: A Robust Fuzzy Descriptor Approach

Van-Anh Nguyen · Anh-Tu Nguyen* · Antoine Dequidt · Laurent Vermeiren · Michel Dambrine

the date of receipt and acceptance should be inserted later

Abstract This paper presents a nonlinear tracking control approach for a two degrees of freedom (2-DoF) serial manipulator. The design goal is to achieve a guaranteed $\mathcal{H}_\infty$ tracking performance while keeping the designed controller as simple as possible for real-time implementation. To this end, the descriptor Takagi-Sugeno fuzzy modeling is used to describe the nonlinear dynamics of the robot. Then, based on Lyapunov stability theory, we propose conditions to design fuzzy controllers for trajectory tracking purposes. The control design procedure is reformulated as an optimization problem under linear matrix inequality constraints which can be effectively solved with semidefinite programming technique. Numerical experiments carried out with the Simscape Multibody™ library of Matlab® clearly demonstrate the effectiveness of the proposed approach in terms of tracking control and numerical simplicity.

Keywords Fuzzy control · Descriptor fuzzy systems · Serial robots · Robot manipulators · Tracking control · Linear matrix inequality (LMI).

1 Introduction

Nowadays, robot manipulators are widely used in all areas of industry for process automation like materials handling, welding, painting, cutting, grinding, etc. These industrial robots have several advantages such as high speed, compactness, accuracy and reliability. For path following applications such as arc welding, laser cutting or machining, one of the most important tasks is to obtain a high-performance tracking of some predefined reference trajectories [1–3]. Tracking control problems are generally considered as more difficult than stabilization or regulation control problems since, in addition to guaranteeing stability of the closed-loop system, specifications on the tracking performance have to be respected for different types of reference trajectories which may be not standard as step or ramps.

Up to now, designing robust tracking controllers for robotics systems is known as a challenging control task [2–6]. This may be explained by several factors. First, robot manipulators have a real nonlinear behaviour. Second, these robots are always subject to uncertain dynamics including unknown friction torques, uncertain inertia, or external disturbances, etc. The latter may limit the practical use of feedback linearization control approach, see for instance [7]. Therefore, a robust control methodology is essential for the tracking control of manipulators. Among the proposed control approaches available in the literature, it can be notably mentioned the sliding mode control theory in [4,8,9], the backstepping control method together with metaheuristic tools in [5], or adaptive control schemes [10–12].

Another approach, more systematic, is the model-based fuzzy control methodology [13–15]. It relies on the use of Takagi-Sugeno (T-S) fuzzy models introduced in [16], which has since then attracted a great attention from academic researchers and engineers, see for instance the following monographs [17–20]. T-S models can be represented by a set of IF-THEN fuzzy rules with consequent parts being local linear representations. They can also be defined in state-space form as convex sums of several local linear submodels with weights called membership functions. They have been proved to constitute a class of universal approximators [21]. In par-

Van-Anh Nguyen · Anh-Tu Nguyen · Antoine Dequidt · Laurent Vermeiren · Michel Dambrine.
Univ. Polytechnique Hauts-de-France, CNRS, UMR 8201-LAMIH, F-59313 Valenciennes, France.
*Corresponding author: Anh-Tu Nguyen.
E-mail: nguyen.trananhtu@gmail.com.

ticular, for sufficiently smooth nonlinear systems, an equivalent representation in T-S fuzzy form can be obtained semiglobally [17].

With the choice of a particular control structure called parallel distributed compensation (PDC) [17] allowing to preserve the convex structure of T-S fuzzy systems, Lyapunov's direct method can be readily applied to derive stability conditions expressed in the form of linear matrix inequalities (LMIs) which can be efficiently solved with available numerical solvers [22]. This approach has been successfully applied to control problems in different fields, including biology [23], transport [22,24], mechatronics [25] and so on. However, one point usually underestimated in most of existing works consists in the complexity inherent to this control approach. Indeed, using the sector nonlinearity approach, the obtained T-S fuzzy model has a number of fuzzy rules which increases *exponentially* with the number of nonlinearities existing in the original nonlinear system [17]. This has several implications that restrict the use of T-S fuzzy control approach to simple manipulators with few degrees of freedom. The first ones is concerned with the control design. Indeed, according to the limitations of actual LMI solvers, no feasible solution can be found to design the feedback control gains, or the computational burden may be too costly that it is impossible to tune correctly the additional control parameters. Another point is that this complexity is echoed in the structure of the control law which reproduces the system one. Hence, more real-time computations are needed for the control, requiring more powerful (and also more costly) processors.

To solve the above control issues, we propose a systematic control framework based on simplified models described as uncertain descriptor T-S fuzzy models. Descriptor T-S fuzzy models were introduced in [17, 26]. For a large class of nonlinear systems including robot manipulators, using the sector nonlinearity approach, the obtained descriptor T-S fuzzy model is much simpler in terms of structure and/or of number of rules than the standard T-S fuzzy model, see for instance [15] for an robotics application. In order to simplify the model complexity, some premise variables can be interpreted as "*modeling uncertainties*". For this class of uncertain descriptor T-S fuzzy models, we propose a new tracking control structure based on the PDC concept in which integral and feedforward actions are integrated to improve the tracking performance. Both feedback and feedforward controller gains can be obtained solving an LMI-based optimization problem to guarantee a predefined level of performance in disturbance attenuation (with a maximal $\mathcal{L}_2$-gain) and in transient response (with a minimal exponential rate).

To illustrate this methodology, we apply it to the tracking control of a 2-DoF serial manipulator. The rest of the paper is organized as follows. The 2-DoF serial manipulator is presented in Section 2 together with a simulation model taking into account the elasticity and the friction of the robot joints. In Section 3, the control model is given and transformed in a descriptor T-S representation. An LMI-based robust control design for fuzzy T-S descriptor system is presented in Section 4. Section 5 presents the control design for the simplified T-S model. Section 6 deals with the application to the tracking control of the 2-DoF serial manipulator. Some numerical experiments are given showing the interests of the proposed approach. Concluding remarks are reported in Section 7.

Notation. Ω_r denotes the number set $\{1, 2, \ldots, r\}$. For a square matrix X, $X^\top$ denotes its transpose, $X > 0$ means that X is positive definite, $X_{(i)}$ denotes its ith row and $\mathrm{He}X = X + X^\top$. $\mathrm{diag}(X_1, X_2)$ denotes a block-diagonal matrix composed of X_1, X_2. I is the identity matrix of appropriate dimension. The symbol "$\star$" stands for the terms deduced by symmetry. The scalar functions $\eta_1, \ldots, \eta_N$ satisfy the convex sum property if $\eta_i \geq 0$ for all $i \in \Omega_r$ and $\sum_{i=1}^{N} \eta_i = 1$. For brevity, we denote $X_h = \sum_{i=1}^{r} h_i X_i$, $Y_{hv} = \sum_{i=1}^{N} \sum_{k=1}^{N_e} h_i v_k Y_{ik}$ and $Z_{hhv} = \sum_{i=1}^{N} \sum_{j=1}^{N} \sum_{k=1}^{N_e} h_i h_j v_k Z_{ijk}$ where X_i, Y_{ik} and Z_{ijk} are matrices of appropriate dimension and the scalar functions h_i and v_k, $i \in \Omega_r$, $k \in \Omega_{N_e}$, of any argument satisfy the convex sum property.

2 System Modeling

This section provides a brief description on the studied serial manipulator, see Fig. 1. For brevity, the system nomenclature used in this work is given in Table 1.

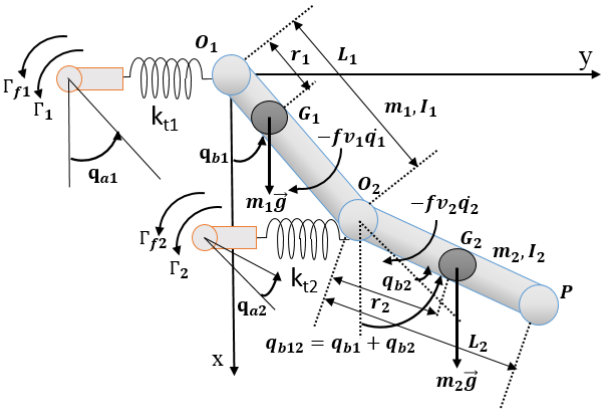

Fig. 1 Description of a 2-DoF robot.

The first arm is of length L_1 and mass m_1 and rotates about the $z-$axis. The second arm, of length L_2 and mass m_2, is attached to the first arm by a revolute joint at point O_2. The rotational angle of first arm, measured clockwise, is denoted q_{b1}, that of second arm q_{b2}, and $q_{b12} = q_{b1}+q_{b2}$. The notations q_{a1} and q_{a2} represent the rotational angles of the first and second actuators. The motor torques are respectively denoted by Γ_1 and Γ_2. To provide more realistic simulations in Section 6, the dynamics induced by the elastic joints [27] between the actuators and the linkages is taken into account in the simulation model, as well as dry friction appearing on revolute joints using Stribeck friction model [28].

The dynamics of the actuator is represented as

$$\Gamma = M_a\ddot{q}_a + N_a\dot{q}_a + \Gamma_t - \Gamma_f, \tag{1}$$

with $q_a = \begin{bmatrix} q_{a1} & q_{a2} \end{bmatrix}^\top$ is the state, $\Gamma_f = \begin{bmatrix} \Gamma_{f1} & \Gamma_{f2} \end{bmatrix}^\top$ is the vector of dry friction torques, $M_a = \mathrm{diag}(I_{a1}, I_{a2})$ is the inertia matrix, and $N_a = \mathrm{diag}(f_{v1}, f_{v2})$ the matrix of viscous friction. The elastic joints are modeled as

$$\Gamma_t = K_t(q_a - q_b) + B_t(\dot{q}_a - \dot{q}_b), \tag{2}$$

where $K_t = \mathrm{diag}(k_{t1}, k_{t2})$, $B_t = \mathrm{diag}(b_{t1}, b_{t2})$ with k_{ti} and b_{ti} are respectively the stiffness and the damping of the ith joint. The friction torques are described by the Stribeck friction model as follows:

$$\Gamma_{fi} = \begin{cases} \Lambda_{ai} & \text{if } |\dot{q}_{ai}| > 0 \text{ (slip)}, \\ \Lambda_{bi} & \text{if } \dot{q}_{ai} = 0 \text{ (stick)}, \end{cases}$$

where

$$\Lambda_{ai} = -\left[\Gamma_{fci} + (\Gamma_{fsi} - \Gamma_{fci})e^{-\left(\frac{\dot{q}_{ai}}{v_s}\right)^2}\right]\mathrm{sign}(\dot{q}_{ai}),$$

$$\Lambda_{bi} = -\min(|\Gamma_i - \Gamma_{ti}|, \Gamma_{fsi})\mathrm{sign}(\Gamma_i - \Gamma_{ti}).$$

Finally, the linkage dynamics are given by

$$\Gamma_t = M_b(q_b)\ddot{q}_b + N_b(q_b, \dot{q}_b)\dot{q}_b + P_b(q_b)q_b, \tag{3}$$

where

$$M_b = \begin{bmatrix} c_1 + 2c_2\cos q_{b2} & c_3 + c_2\cos q_{b2} \\ c_3 + c_2\cos q_{b2} & c_3 \end{bmatrix},$$

$$N_b = \begin{bmatrix} 2c_2\dot{q}_{b2}\sin q_{b2} & c_2\dot{q}_{b2}\sin q_{b2} \\ -c_2\dot{q}_{b1}\sin q_{b2} & 0 \end{bmatrix},$$

$$P_b = \begin{bmatrix} -c_4\frac{\sin q_{b1}}{q_{b1}} - c_5\frac{\sin q_{b12}}{q_{b12}} & -c_5\frac{\sin q_{b12}}{q_{b12}} \\ -c_5\frac{\sin q_{b12}}{q_{b12}} & -c_5\frac{\sin q_{b12}}{q_{b12}} \end{bmatrix},$$

with $c_1 = m_1r_1^2 + I_1 + m_2L_1^2 + m_2r_2^2 + I_2$, $c_2 = m_2L_1r_2$, $c_3 = m_2r_2^2 + I_2$, $c_4 = m_1gr_1 + m_2gL_1$, $c_5 = m_2gr_2$. It should be noted that the above serial manipulator model has 4-DoF, *i.e.*, two from the actuators and two others for the robot arms. The system modeling includes the transmission deformation between an actuator and its corresponding arm [29]. This additional and weakly damped dynamics introduces vibrations due to the excitation of the mechanical resonances resulting from the deformations. However, for control purposes, we assume that the actuator positions q_{a1} and q_{a2} coincide with the arm positions q_{b1} and q_{b2}. As a consequence, the nonlinear dynamics can be computed from (1), (2) and (3) with $q = q_a = q_b$ in the following form:

$$\Gamma = M(q)\ddot{q} + N(q, \dot{q})\dot{q} + P(q)q - \Gamma_f, \tag{4}$$

with $M = M_a + M_b$, $N = N_a + N_b$, $P = P_b$. In the following section, an equivalent representation in a fuzzy descriptor form of model (4) is presented.

Table 1 System Nomenclature.

Symbol	Description	Value
$L_1,\ L_2$	Lengths of robot arms (m)	0.5, 0.5
$m_1,\ m_2$	Masses of robot arms (kg)	15, 9
$I_1,\ I_2$	Inertia of robot arms (kgm^2)	0.31, 0.19
$r_1,\ r_2$	Distances between joint axis and mass center (m)	0.25, 0.25
$f_{v1},\ f_{v2}$	Coefficients of viscous friction (Nms/rd)	0.14, 0.14
g	Gravity acceleration (m/s^2)	9.81
$I_{a1},\ I_{a2}$	Actuator inertia (kgm^2)	2.71, 0.50
$k_{t1},\ k_{t2}$	Stiffness constant $\times 10^4$(N/m)	6.4, 1.2
$b_{t1},\ b_{t2}$	Damping constant (Ns/m)	20.4, 3.8
$\Gamma_{fs1},\ \Gamma_{fs2}$	Static friction torque (Nm)	6, 3
$\Gamma_{fc1},\ \Gamma_{fc2}$	Coulomb friction torque (Nm)	4, 2
v_s	Sliding speed coefficient (m/s)	0.1

3 System Description and Reference Model

This section provides a new representation of the considered serial manipulator and define the reference model corresponding to the desired dynamical behaviour of the system. To this end, let us define the state vector as $x_p = [q_1\ q_2\ \dot{q}_1\ \dot{q}_2]^\top \in \mathbb{R}^{n_x}$, the input vector $u = [\Gamma_1\ \Gamma_2]^\top \in \mathbb{R}^{n_u}$, the controlled output vector $y = [q_1\ q_2]^\top$, and the disturbance vector $d = \Gamma_f \in \mathbb{R}^{n_d}$. The dynamics of the manipulator (4) can be represented in the following regular descriptor form:

$$\begin{aligned} E_p(z)\dot{x}_p(t) &= A_p(z)\,x_p(t) + B_p\,u(t) + B_d\,d(t), \\ y(t) &= C_p x_p(t), \end{aligned} \tag{5}$$

where

$$E_p(z) = \begin{bmatrix} 1 & 0 & 0 & 0 \\ 0 & 1 & 0 & 0 \\ 0 & 0 & \hat{I}_{a1} + 2c_2 z_1 & c_3 + c_2 z_1 \\ 0 & 0 & c_3 + c_2 z_1 & \hat{I}_{a2} \end{bmatrix}, \quad C_p = \begin{bmatrix} 1 & 0 \\ 0 & 1 \\ 0 & 0 \\ 0 & 0 \end{bmatrix}^\top,$$

$$A_p(z) = \begin{bmatrix} 0 & 0 & 1 & 0 \\ 0 & 0 & 0 & 1 \\ z_2 & z_3 & 2z_4 - f_{v1} & z_4 \\ z_3 & z_3 & z_5 & -f_{v2} \end{bmatrix}, \quad B_p = B_d = \begin{bmatrix} 0 & 0 \\ 0 & 0 \\ 1 & 0 \\ 0 & 1 \end{bmatrix},$$

with $\hat{I}_{a1} = I_{a1} + c_1$, $\hat{I}_{a2} = I_{a2} + c_3$ and

$$z_1 = \cos q_2,\ z_2 = -c_4 \mathrm{sinc} q_1 - c_5 \mathrm{sinc} q_{12}, \qquad (6)$$
$$z_3 = -c_5 \mathrm{sinc} q_{12},\ z_4 = c_2 \dot{q}_2 \sin q_2,\ z_5 = -c_2 \dot{q}_1 \sin q_2.$$

By applying the sector nonlinear approach [17,26], the following T-S fuzzy representation can be derived:

$$\begin{aligned} E_{pv}\dot{x}_p(t) &= A_{ph}x_p(t) + B_{ph}u(t) + B_d\, d(t), \\ y(t) &= C_p x(t), \end{aligned} \qquad (7)$$

where

$$E_{pv} = \sum_{k=1}^{N_e} v_k(z)(E_{pk}),\ [A_{ph}\ B_{ph}] = \sum_{i=1}^{N} h_i(z)[A_{pi}\ B_{pi}].$$

Note that the T-S fuzzy descriptor system (7) is an *equivalent* form of (5) in a given bounded subset of the state space. The construction of this model is given in more details in Section 6.1. It can be shown that the matrix E_{pv} is non-singular for all z. To guarantee a desired tracking performance, we consider the following reference model:

$$\dot{x}_r(t) = A_r x_r(t) + B_r r(t), \qquad (8)$$

where $x_r(t) \in \mathbb{R}^{n_x}$ is the reference state to be followed by the robot state $x_p(t)$ and $r(t) \in \mathbb{R}^{n_r}$ is the bounded reference input. The matrices A_r and B_r are designed according to the desired closed-loop dynamics of the serial manipulator. The tracking error is defined by

$$e(t) = x_p(t) - x_r(t).$$

From (7) and (8), the following tracking error dynamics can be obtained:

$$\begin{aligned} E_{pv}\dot{e}(t) = A_{ph}e(t) + (A_{ph} - E_{pv}A_r)x_r(t) \\ + B_{ph}u(t) - E_{pv}B_r r(t) + B_d d(t). \end{aligned} \qquad (9)$$

Defining the augmented state vector $x(t) = [e(t)^\top\ x_r(t)^\top]^\top$ and the exogenous input vector $w(t) = [d(t)^\top\ r(t)^\top]^\top$, the two dynamics (8) and (9) can be now gathered in the following regular descriptor representation:

$$E_v\dot{x}(t) = A_{hv}x(t) + B_h u(t) + D_v w(t), \qquad (10)$$

where

$$E_v = \begin{bmatrix} E_{pv} & 0 \\ 0 & I \end{bmatrix}, \quad D_v = \begin{bmatrix} B_d & -E_{pv}B_r \\ 0 & B_r \end{bmatrix}, \qquad (11)$$
$$B_h = \begin{bmatrix} B_{ph} \\ 0 \end{bmatrix}, \quad A_{hv} = \begin{bmatrix} A_{ph} & A_{ph} - E_{pv}A_r \\ 0 & A_r \end{bmatrix}.$$

Next, the descriptor system (10) will be used to design a tracking controller for the studied manipulator robot.

4 Tracking Control for Descriptor Fuzzy Systems

4.1 Design Specifications

We consider the class of controllers given by

$$\begin{aligned} u(t) &= \sum_{i=1}^{N}\sum_{k=1}^{N_e} h_i(z)v_k(z)\left(K_{ik}e(t) + L_{ik}r(t)\right) \\ &= [K_{hv}\ 0]\, x(t) + [0\ L_{hv}]\, w(t). \end{aligned} \qquad (12)$$

Our control goal is to determine the gain matrices K_{ik} and L_{ik} of controller (12) such that system (10) verifies the following closed-loop performance specifications.

- (*Asymptotic stability*). For $w(t) = 0$, the zero solution of the closed-loop system (7) under the control effect of (12) is asymptotically stable.
- (*Decay rate performance*). Given a positive scalar α and for $w(t) = 0$, the tracking error $e(t)$ converges exponentially towards the origin with a decay rate less than α.
- ($\mathcal{H}_\infty$ *tracking performance*). Given a positive definite matrix Q and a positive scalar γ, the inequality

$$\int_0^{t_f} e(t)^\top Q e(t) dt \le \gamma^2 \int_0^{t_f} w(t)^\top w(t) dt \qquad (13)$$

holds for any $t_f > 0$, and zero initial conditions.

Remark 1 Inequality (13) implies that if $w(t)$ is a energy-bounded signal ($w(t) \in \mathcal{L}_2$) then, the same holds for the tracking error, *i.e.*, $e(t) \in \mathcal{L}_2$. The coefficient γ is called a bound for the $\mathcal{L}_2-$gain of the system. The smaller γ is, the more accurate is the following of the reference trajectory. Note that matrix Q, usually taken as an identity matrix [30], allows additional degree-of-freedom in the control design.

Remark 2 An integral action can be easily introduced in the control law to achieve a zero error in steady state for a constant exogenous input $w(t)$ by considering an additional state vector $x_I(t)$ equals to the integral of

the output tracking error, *i.e.*, $\dot{x}_I(t) = C_p e(t)$. Denoting $\bar{x}(t) = [e^\top \; x_I^\top \; x_r^\top]^\top$, the control law becomes

$$\begin{aligned} u(t) &= K_{hv} e(t) + H_{hv} x_I(t) + L_{hv} r(t) \\ &= [\bar{K}_{hv} \; 0]\, \bar{x}(t) + [0 \; L_{hv}]\, w(t), \end{aligned}$$

where $\bar{K}_{hv} = [K_{hv} \; H_{hv}]$, while, in the system description (10) and (11), matrix E_{pv} should be replaced by $\mathrm{diag}(E_{pv}, I)$, matrix A_{ph} by

$$\begin{bmatrix} A_{ph} & 0 & A_{ph} - E_{pv} B_r \\ C_p & 0 & 0 \\ 0 & 0 & A_r \end{bmatrix},$$

and so on.

4.2 LMI-Based Control Design Conditions

LMI-based constraints allowing the computation of the control gain matrices K_{ik} and L_{ik} are given in the following theorem.

Theorem 1 *If there exist $n_x \times n_x$-matrices $P_{11} > 0$, $P_{22} > 0$, Q_{11ij}, Q_{12ij}, Q_{21ij}, Q_{22ij}, X_{11ij}, X_{12ij}, X_{21ij}, X_{22ij}, matrices $M_{jk} \in \mathbb{R}^{n_u \times n_x}$, $L_{jk} \in \mathbb{R}^{n_u \times n_r}$, and a positive scalar γ such that*

$$\Xi_{iik} < 0, \quad \Xi_{ijk} + \Xi_{jik} < 0, \tag{14}$$

where $\forall i, j \in \Omega_r$, $i < j$ and $k \in \Omega_{N_e}$. The block matrix Ξ_{ijk} is defined as

$$\Xi_{ijk} = \begin{bmatrix} S_{11} & \star & \star & \star & \star & \star & \star \\ S_{21} & S_{22} & \star & \star & \star & \star & \star \\ S_{31} & S_{32} & S_{33} & \star & \star & \star & \star \\ S_{41} & S_{42} & S_{43} & S_{44} & \star & \star & \star \\ 0 & 0 & B_d^T & 0 & -\gamma^2 I & \star & \star \\ 0 & 0 & S_{63} & B_r^T & 0 & -\gamma^2 I & \star \\ P_{11} & 0 & 0 & 0 & 0 & 0 & -Q^{-1} \end{bmatrix}, \tag{15}$$

and

$$\begin{aligned} &S_{11} = \mathrm{He}(Q_{11ij} + \alpha P_{11}), \; S_{21} = Q_{21ij} + Q_{12ij}^\top, \\ &S_{31} = A_{pi} P_{11} + B_{pi} M_{jk} - E_{pk} Q_{11ij} + X_{11ij}^\top, \\ &S_{41} = -Q_{21ij} + X_{12ij}^\top, \; S_{22} = \mathrm{He}(Q_{22ij} + \alpha P_{22}), \\ &S_{32} = (A_{pi} - E_{pk} A_r) P_{22} - E_{pk} Q_{12ij} + X_{21ij}^\top, \\ &S_{42} = A_r P_{22} - Q_{22ij} + X_{22ij}^\top, \\ &S_{43} = -X_{21ij} - X_{12ij}^\top E_{pk}^\top, \quad S_{44} = -\mathrm{He}(X_{22ij}), \\ &S_{33} = -\mathrm{He}(E_{pk} X_{11ij}), \; S_{63} = (B_{pi} L_{jk})^T - (E_{pk} B_r)^T. \end{aligned}$$

Then, the control law (12) with $K_{ik} = M_{ik} P_{11}^{-1}$ and L_{ik} is such that the specifications given in Section 4.1 are satisfied.

Proof Using the extended state vector $x^* = [x^\top \; \dot{x}^\top]^\top$, the closed-loop system can be represented in a singular descriptor form:

$$\mathbb{E}^* \dot{x}^* = \mathbb{A}_{hhv}^* x^* + \mathbb{B}_{hv}^* w, \tag{16}$$

where

$$\mathbb{E}^* = \begin{bmatrix} I & 0 \\ 0 & 0 \end{bmatrix}, \; \mathbb{A}_{hhv}^* = \begin{bmatrix} 0 & I \\ \mathbb{A}_{hhv} & -E_v \end{bmatrix}, \; \mathbb{B}_{hv}^* = \begin{bmatrix} 0 \\ \mathbb{B}_{hv} \end{bmatrix},$$

$$\mathbb{A}_{hhv} = A_{hv} + B_h [K_{hv} \; 0], \; \mathbb{B}_{hv} = D_v + B_h [0 \; L_{hv}].$$

Let us define

$$\mathbb{P}_{hh}^* = \begin{bmatrix} \mathbb{P} & 0 \\ \mathbb{Q}_{hh} & \mathbb{X}_{hh} \end{bmatrix}, \quad \mathbb{P} = \begin{bmatrix} P_{11} & 0 \\ 0 & P_{22} \end{bmatrix}, \tag{17}$$

where $\mathbb{Q}_{hh} = \begin{bmatrix} Q_{11hh} & Q_{12hh} \\ Q_{21hh} & Q_{22hh} \end{bmatrix}$, $\mathbb{X}_{hh} = \begin{bmatrix} X_{11hh} & X_{12hh} \\ X_{21hh} & X_{22hh} \end{bmatrix}$. From the definition of Ξ_{ijk} in (15), some simple computations lead to

$$\Xi_{hhv} = \begin{bmatrix} \Xi_{11} & \star & \star \\ \mathbb{B}_{hv}^{*\top} & -\gamma^2 I & 0 \\ C_z^* \mathbb{P}_{hh}^* & 0 & -Q^{-1} \end{bmatrix}, \tag{18}$$

where $C_z^* = [I \; 0 \; 0 \; 0]$ and $\Xi_{11} = \mathrm{He}(\mathbb{P}_{hh}^{*\top} \mathbb{A}_{hv}^{*\top} + \alpha \mathbb{P}_{hh}^{*\top} \mathbb{E}^*)$. Since the membership functions satisfy the convex sum property, it follows from conditions (14) that

$$\Xi_{hhv} < 0. \tag{19}$$

Note that Ξ_{11} can be represented in the form

$$\Xi_{11} = \begin{bmatrix} \mathrm{He}(\mathbb{Q}_{hh} + \alpha \mathbb{P}) & \star \\ \mathbb{A}_{hv} \mathbb{P} - E_v \mathbb{Q}_{hh} + \mathbb{X}_{hh}^\top & -\mathrm{He}(E_v \mathbb{X}_{hh}) \end{bmatrix}.$$

Inequality (19) leads to $\mathrm{He}(E_v \mathbb{X}_{hh}) > 0$. As a consequence, $\mathbb{X}_{hh}$ and $\mathbb{P}_{hh}^*$ are non-singular matrices since E_v is non-singular. Consider the following Lyapunov function candidate:

$$V(x^*) = x^{*\top} \mathbb{E}^* \mathbb{P}_{hh}^{*-1} x^*.$$

The derivative of the function V along the trajectories of (16) is given by

$$\dot{V}(x^*) = \dot{x}^{*\top} \mathbb{E}^* \mathbb{P}_{hh}^{*-1} x^* + x^{*\top} \mathbb{P}_{hh}^{*-\top} \mathbb{E}^* \dot{x}^*. \tag{20}$$

Note that due to the special structure of $\mathbb{P}_{hh}^*$ in (17), one has $\mathbb{E}^{*T} \dot{\mathbb{P}}_{hh}^{*^{-1}} = 0$. This means that there are no time-derivatives of the membership functions in the expression of $\dot{V}$. It should be noted that dealing with *unknown* time-derivatives of the membership functions in the T-S fuzzy control framework still remains an open research issue, see [31–33].

From (16) and (20), we can obtain the equality

$$\dot{V}(x^*) + e^\top Q e - \gamma^2 w^\top w + 2\alpha V(x^*) = \xi^\top \Omega_{hhv} \xi,$$

where

$$\xi = \begin{bmatrix} \mathbb{P}_{hh}^{*-1} x^* \\ w \end{bmatrix},\ \Omega_{hhv} = \begin{bmatrix} \Xi_{11} + \mathbb{P}_{hh}^{*\top} C_z^{*\top} Q C_z^* \mathbb{P}_{hh}^* & \star \\ \mathbb{B}_{hv}^{*\top} & -\gamma^2 I \end{bmatrix}.$$

By Schur complement lemma, we can show that (19) is equivalent to $\Omega_{hhv} < 0$. This means that

$$\dot{V}(x^*) + e^\top Q e - \gamma^2 w^\top w + 2\alpha V(x^*) < 0. \tag{21}$$

By standard arguments, the properties of the closed-loop system can then be easily established.

5 Complexity Reduction for Real-Time Control

5.1 Reduction of Fuzzy Rules

This section presents a way to reduce the number of rules for the generalized form T-S fuzzy systems. The rule reduction is related to the computational effort for controller design utilizing LMIs. To deal with this problem, some nonlinearities appearing in the initial model (5) are considered as parameter uncertainties. Applying again the sector nonlinear approach, an uncertain descriptor T-S representation can be derived:

$$\begin{aligned} \hat{E}_{pv}\dot{x}_p(t) &= \hat{A}_{ph}x_p(t) + \hat{B}_{ph}u(t) + B_d\, d(t), \\ y(t) &= C_h x(t), \end{aligned} \tag{22}$$

where

$$\hat{E}_{pv} = \sum_{k=1}^{N_e} v_k(z)(E_{pk} + \Delta E_{pk}),$$

$$[\hat{A}_{ph}\ \hat{B}_{ph}] = \sum_{i=1}^{N} h_i(z)[A_{pi} + \Delta A_{pi}\ B_{pi} + \Delta B_{pi}].$$

The system uncertainties can be represented in the form

$$\begin{aligned} &\Delta E_{pk} = H_e^\top \Delta_e W_{epk},\ \Delta A_{pi} = H_a^\top \Delta_a W_{api}, \\ &\Delta B_{pi} = H_b^\top \Delta_b W_{bpi},\ k \in \Omega_{N_e},\ i \in \Omega_r, \end{aligned}$$

where $\Delta_\ell^\top \Delta_\ell(t) \le I$ with $\ell \in \{e, a, b\}$.

5.2 LMI-Based Robust Control Design Conditions

The following theorem provides LMI conditions to design a robust PDC controller (12) for the uncertain descriptor system (22).

Theorem 2 *If there exist $n_x \times n_x$-matrices $P_{11} > 0$, $P_{22} > 0$, Q_{11ij}, Q_{12ij}, Q_{21ij}, Q_{22ij}, X_{11ij}, X_{12ij}, X_{21ij}, X_{22ij}, matrices $M_{jk} \in \mathbb{R}^{n_u \times n_x}$, $L_{jk} \in \mathbb{R}^{n_u \times n_r}$, and positive scalars γ, τ_{ijk}^a, τ_{ijk}^b, τ_{ijk}^e such that*

$$\Psi_{iik} < 0, \quad \Psi_{ijk} + \Psi_{jik} < 0, \tag{23}$$

where $\forall i, j \in \Omega_r$, $i < j$ and $k \in \Omega_{N_e}$. The block matrix Ψ_{ijk} is defined as

$$\Psi_{ijk} = \begin{bmatrix} \Psi_{1ijk} & \star \\ \Psi_{2ijk} & \Psi_{3ijk} \end{bmatrix},$$

with

$$\Psi_{1ijk} = \begin{bmatrix} S_{11} & \star & \star & \star & \star & \star & \star \\ S_{21} & S_{22} & \star & \star & \star & \star & \star \\ S_{31} & S_{32} & S_{33}^* & \star & \star & \star & \star \\ S_{41} & S_{42} & S_{43} & S_{44} & \star & \star & \star \\ 0 & 0 & B_d^\top & 0 & -\gamma^2 I & \star & \star \\ 0 & 0 & S_{63} & B_r^\top & 0 & -\gamma^2 I & \star \\ P_{11} & 0 & 0 & 0 & 0 & 0 & -Q^{-1} \end{bmatrix},$$

$$\Psi_{2ijk} = \begin{bmatrix} T_{11} & T_{12} & 0 & 0 & 0 & 0 & 0 \\ T_{21} & 0 & 0 & 0 & 0 & T_{26} & 0 \\ T_{31} & T_{32} & T_{33} & T_{34} & 0 & T_{36} & 0 \end{bmatrix},$$

$$\Psi_{3ijk} = \mathrm{diag}(-\tau_{ijk}^a I, -\tau_{ijk}^b I, -\tau_{ijk}^e I),$$

where

$$\begin{aligned} S_{33}^* =& S_{33} + \tau_{ijk}^a H_a^\top H_a + \tau_{ijk}^b H_b^\top H_b + \tau_{ijk}^e H_e^\top H_e, \\ T_{11} =& W_{api} P_{11}, \quad T_{21} = W_{bpi} M_{jk}, \\ T_{31} =& -W_{epk} Q_{11ij}, \quad T_{12} = W_{api} P_{22}, \\ T_{32} =& -W_{epk}(A_r P_{22} - Q_{12ij}),\ T_{33} = -W_{epk} X_{11ij}, \\ T_{34} =& -W_{epk} X_{12ij},\ T_{26} = W_{bpi} L_{jk},\ T_{36} = -W_{epk} B_r. \end{aligned}$$

Then, the control law (12) with $K_{ik} = M_{ik} P_{11}^{-1}$ and L_{ik} is such that the specifications given in Section 4.1 are satisfied for the uncertain case.

Proof Following the same line as in the proof of Theorem 1, we can prove that (21) is satisfied if

$$\hat{\Xi}_{hhv} = \Xi_{hhv} + \Delta\Xi_{hhv} < 0,$$

where Ξ_{hhv} is defined in (18). The uncertain term $\Delta\Xi_{hhv}$ is defined as follows:

$$\Delta\Xi_{hhv} = \bar{H}^\top \Delta(t) \Psi_{2hhv} + \Psi_{2hhv}^\top \Delta(t)^\top \bar{H},$$

where

$$\begin{aligned} \Delta(t) &= \mathrm{diag}(\Delta_a(t), \Delta_b(t), \Delta_e(t)), \\ \bar{H} &= \begin{bmatrix} 0 & 0 & H_a & 0 & 0 & 0 & 0 \\ 0 & 0 & H_b & 0 & 0 & 0 & 0 \\ 0 & 0 & H_e & 0 & 0 & 0 & 0 \end{bmatrix}. \end{aligned}$$

Let $S_{hhv} = -\Psi_{3hhv} > 0$. By completion of squares, it follows easily that

$$\begin{aligned} \Xi_{hhv} + \Delta\Xi_{hhv} &\le \Xi_{hhv} + \bar{H}^\top S_{hhv} \bar{H} \\ &\quad + \Psi_{2hhv}^\top \Delta(t)^\top S_{hhv}^{-1} \Delta(t) \Psi_{2hhv} \\ &\le \Xi_{hhv} + \bar{H}^\top S_{hhv} \bar{H} + \Psi_{2hhv}^\top S_{hhv}^{-1} \Psi_{2hhv}. \end{aligned}$$

By Schur complement lemma, it can be easily shown that $\Xi_{hhv} + \Delta\Xi_{hhv} < 0$ if $\Psi_{hhv} < 0$. This latter is ensured by inequalities (23), which completes the proof.

Remark 3 A large value of the guaranteed decay rate α or a small value of the $\mathcal{H}_\infty$ gain γ may lead to unacceptable control gain. This problem can be easily dealt with in the feedback design by introducing additional LMI constraints in the optimization problem. The decision variable M_{ik} is linked with the control gains by the expression $M_{ik} = K_{ik}P_{11}$. To prevent *excessively* high feedback gains, it can be imposed that

$$M_{ik}M_{ik}^\top \leq \epsilon^2 I_{n_u}, \quad i \in \Omega_N,\ k \in \Omega_{N_e}, \tag{24}$$

for some positive scalar ϵ. Condition (24) is equivalent to the following LMIs:

$$\begin{bmatrix} \epsilon^2 I_{n_u} & M_{ik} \\ M_{ik}^\top & I_{n_x} \end{bmatrix} \geq 0, \quad i \in \Omega_N,\ k \in \Omega_{N_e}.$$

Remark 4 The computational complexity of the LMI-based optimizations can be evaluated by the number of scalar decision variables $\mathcal{N}_{var}$ and the number of rows of all considered LMI conditions $\mathcal{N}_{row}$. These numbers corresponding to Theorem 1 are given by

$$\mathcal{N}_{var} = 6 + n_x(1 + 3N^2 + N_eN^2 + n_d),$$
$$\mathcal{N}_{row} = 6n_x(1 + NN_e) + n_xN(8n_xN + N_en_u).$$

Therefore, we can reduce the computational complexity by reducing the number of rules N and N_e.

6 Application to Robot Fuzzy Tracking Control

The T-S fuzzy descriptor control approach is applied in the following for the trajectory tracking of the 2-DoF robot. Numerical results obtained with the simulation robot model presented in Section 2 are then provided to demonstrate the practical performance of the proposed tracking controllers.

6.1 Fuzzy Descriptor Modeling for Tracking Control

The following joint limitations are considered for the studied 2-DoF manipulator:

$$\begin{aligned} &|q_1| \leq \pi \text{ rad}, && |q_2| \leq \pi \text{ rad}, \\ &|\dot{q}_1| \leq 15 \text{ rad/s}, && |\dot{q}_2| \leq 15 \text{ rad/s}. \end{aligned} \tag{25}$$

The above limits are defined such that the serial robot can operate in a large workspace while taking into account its physical characteristics.

6.1.1 Exact Fuzzy Descriptor Representation

The premise variables z_i defined in (6) are bounded on the subset defined by (25). Let $z_{i\min}$ and $z_{i\max}$ be respectively the lower and upper bounds of the premise z_i on that subset. Using the parameter values given in Table 1, it can be obtain the following bounds:

$$z_{1\max} = -z_{1\min} = 1,\ z_{2\max} = z_{3\max} = 4.79,$$
$$z_{2\min} = -103.01,\ z_{3\min} = -22.07,$$
$$z_{4\max} = z_{5\max} = -z_{4\min} = -z_{5\min} = 16.87.$$

Using the sector nonlinearity approach [17], an *exact* T-S fuzzy descriptor representation for the control-based robot model (5) can be easily obtained. The derivation of this $2^5 = 32$ rules T-S fuzzy representation is standard and omitted here due to the space limitation.

6.1.2 Fuzzy Modeling with Reduced Complexity

Theoretically, the control approach proposed in Section 4 can be used to deal with T-S descriptor systems with any number of rules. However, a large number of rules may cause costly computational burden for real-time control implementation. Therefore, it is worth simplifying the T-S fuzzy model to cope with the hardware limitations. To achieve this goal, some system nonlinearities will be considered as modeling uncertainties in order to reduce the number of premise variables, and thus the number of submodels. Then, these uncertainties can be dealt with using the robust control scheme proposed in Theorem 2. We present here an example leading to a T-S fuzzy system with 8 rules from system (22). To this end, we consider

$$z_4(t) = z_{4\max}f_1(t), \quad z_5(t) = z_{5\max}f_2(t),$$

with $|f_i(t)| \leq 1$, $i = 1, 2$. Let us define

$$\omega_{i1} = \frac{z_i - z_{i\min}}{z_{i\max} - z_{i\min}}, \quad \omega_{i2} = 1 - \omega_{i1}, \quad i \in \Omega_3.$$

The membership functions of the above T-S fuzzy descriptor system are expressed as follows:

$$v_1(z) = \omega_{11}, \quad h_1(z) = \omega_{21}\omega_{31}, \quad h_2(z) = \omega_{22}\omega_{31},$$
$$v_2(z) = \omega_{12}, \quad h_3(z) = \omega_{21}\omega_{32}, \quad h_4(z) = \omega_{22}\omega_{32}.$$

Then, the model (5) can be represented in the form (22) with the nominal matrices given by

$$E_{p1} = E_p(z_{1\min}), \quad E_{p2} = E_p(z_{1\max}),$$
$$A_{p1} = A_p(z_{2\min}, z_{3\min}), \quad A_{p2} = A_p(z_{2\max}, z_{3\min}),$$
$$A_{p3} = A_p(z_{2\min}, z_{3\max}), \quad A_{p4} = A_p(z_{2\max}, z_{3\max}),$$
$$B_{pi} = B_p, \quad i \in \Omega_4,$$

and

$$\Delta E_{pv} = 0,\ \Delta B_{ph} = 0,\ \Delta_{pa} = \mathrm{diag}(f_1(t), f_2(t)),$$
$$H_a = \begin{bmatrix} 0\ 0\ 1\ 0 \\ 0\ 0\ 0\ 1 \end{bmatrix}, \quad W_{aph} = \begin{bmatrix} 0\ 0\ 2z_{4\max}\ z_{4\max} \\ 0\ 0\ \ z_{5\max}\ \ 0 \end{bmatrix}.$$

Observe that the obtained nonlinear uncertain descriptor system has now only 3 premise variables $z_1(t)$, $z_2(t)$ and $z_3(t)$, and so $2^3 = 8$ rules. Similarly, we can obtain a 4-rules (respectively 2-rules) T-S fuzzy model by considering $z_2(t)$, $z_4(t)$, $z_5(t)$ (respectively $z_1(t)$, $z_2(t)$, $z_4(t)$, $z_5(t)$) as system uncertainties. It is clear that a *linear* uncertain descriptor system can be easily obtained following the same line while considering all premise variables as model uncertainties. The details of these uncertain T-S fuzzy descriptor systems are not given here for brevity.

6.1.3 Tracking Reference Model

The coordinates of the effector position $\mathbf{P}$ in the $xy-$plane are expressed by the forward kinematic model as follows, see Fig. 1:

$$x_P = L_1 \cos(q_1) + L_2 \cos(q_1 + q_2), \qquad (26)$$
$$y_P = L_1 \sin(q_1) + L_2 \sin(q_1 + q_2).$$

It is desired that the point $\mathbf{P}$ follows a *circular* trajectory reference with a radius of $R = 0.2$ m and a center defined as $x_{P0} = 0.35$ m, $y_{P0} = 0.65$ m. The corresponding position of $\mathbf{P}$ at time t is given as

$$x_P(t) = x_{P0} + R\cos\psi(t), \quad y_P(t) = y_{P0} + R\sin\psi(t),$$

where $\psi(t)$ is defined as a quintic polynomial so that the circular trajectory is executed in a duration of 1.5 s with a maximum curvilinear velocity of 1.57 m/s. The desired angular positions $q_{1d}(t)$ and $q_{2d}(t)$ are computed using the inverse kinematic model derived from the forward one (26). The state-space matrices of the reference model (8) are given as follows:

$$A_r = \begin{bmatrix} 0 & 0 & 1 & 0 \\ 0 & 0 & 0 & 1 \\ -3844 & 0 & -124 & 0 \\ 0 & -3844 & 0 & -124 \end{bmatrix},$$
$$B_r = \begin{bmatrix} 0 & 0 & 0 & 0 & 0\ 0 \\ 0 & 0 & 0 & 0 & 0\ 0 \\ 3844 & 0 & 124 & 0 & 1\ 0 \\ 0 & 3844 & 0 & 124 & 0\ 1 \end{bmatrix}.$$

This corresponds to two decoupled, second-order dynamics with a real double pole located at -62 rad/s to avoid the excitation of unmodeled high-frequency dynamics which appears in the simulation model (1)-(3). The reference model input is defined as

$$r(t) = \left[q_{1d}(t)\ q_{2d}(t)\ \dot{q}_{1d}(t)\ \dot{q}_{2d}(t)\ \ddot{q}_{1d}(t)\ \ddot{q}_{2d}(t)\right].$$

This choice allows guaranteeing a sufficiently *smoothness* level for the reference trajectory. The detail is omitted here since the reference design is out of the scope of this paper.

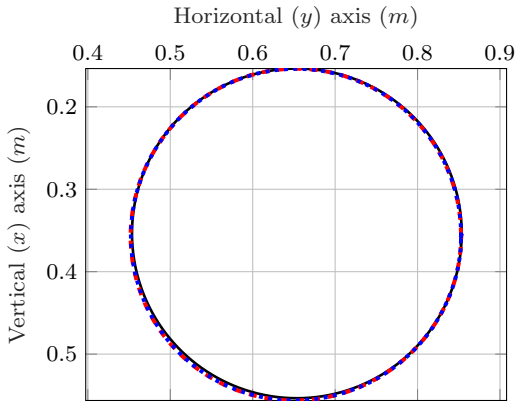

Fig. 2 End-effector trajectories for Case 1. Reference (solid black), trajectory with 32-rules controller (dotted blue), trajectory with 4-rules controller (dashed red).

6.2 Illustrative Results and Discussions

This section provides numerical results carried out with the robot simulation model presented in Section 2 embedded in Simscape Multibody$^{\mathrm{TM}}$ environment of Matlab/Simulink software. For tracking purposes, an integral action is incorporated in the PDC control scheme as explained in Remark 2. All LMI problems are solved with Matlab using the Yalmip Toolbox [34] and the solver SDPT3 [35]. A comparative study between two tracking controllers derived from a full T-S fuzzy representation and a simplified one is given to emphasize the interest of the proposed robust control scheme for real-time applications. It should be stressed also that when solving LMI conditions in Theorem 2, feasible solutions can only be obtained with T-S fuzzy descriptor models having at least 4 rules. This means that a trade-off between the complexity of the model and the design conservatism has to be found.

To demonstrate the robustness of the proposed approach, a comparison between results obtained for three cases is provided. The first case (Case 1) is the nominal one in which the robot is unloaded and free of contact. The second one (Case 2) occurs during a machining process. In this case, the external disturbance corresponds

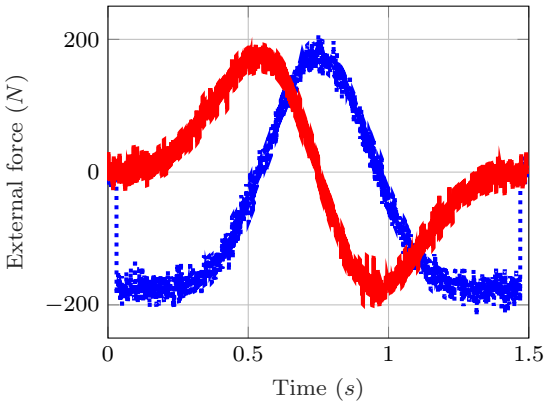

Fig. 3 External force. Vertical (dotted blue) and horizontal (solid red) components during circular trajectory.

to an external force $F_e(t)$ tangential to the effector trajectory applied on it

$$F_e(t) = -f_e(t)\frac{\dot{\varrho}(t)}{||\varrho(t)||},$$

with $\varrho(t) = [\dot{x}_P \ \dot{y}_P]^\top$ and $f_e(t) \in [138, 218]$ N, see Fig. 3. For the last case (Case 3), the robot manipulator must carry a mass of 5 kg. This corresponds to a variation of the effector mass m_2 of 55.6%. Note that, as explained in Section 2, in all these cases, the friction and joint elasticity effects are taken into account in the simulation, although not considered in the control model.

For illustration, we take the case of a 4-rules uncertain T-S fuzzy descriptor model obtained by considering $z_2(t)$, $z_4(t)$ and $z_5(t)$ as system uncertainties. Solving the LMI conditions in Theorem 2 for this case gives control gains with very high values, see for instance

$$K_{11} = 10^9 \times \begin{bmatrix} 3.88 & 0.15 & 0.03 & 0.01 \\ 0.20 & 7.89 & 0.01 & 0.08 \end{bmatrix},$$
$$H_{11} = 10^9 \times \begin{bmatrix} -3.88 & -0.15 \\ -0.21 & -7.89 \end{bmatrix},$$
$$K_{12} = 10^8 \times \begin{bmatrix} 8.12 & -0.03 & 0.08 & -0.01 \\ -0.04 & 0.01 & -0.01 & 0.01 \end{bmatrix},$$
$$H_{12} = 10^8 \times \begin{bmatrix} -8.13 & 0.03 \\ 0.04 & -0.01 \end{bmatrix}.$$

It is clear that such control gains are impractical for real-time implementation. Hence, we redesign the feedback gains by including the additional constraint (24) with $\epsilon = 10^4$ as explained in Remark 3. The following control results are obtained

$$K_{11} = 10^4 \times \begin{bmatrix} -6.31 & 1.16 & -0.0978 & -0.0018 \\ 0.91 & -6.513 & 0.0044 & -0.0591 \end{bmatrix},$$
$$H_{11} = 10^4 \times \begin{bmatrix} 0.720 & 0.939 \\ 0.939 & 4.62 \end{bmatrix},$$
$$K_{12} = 10^3 \times \begin{bmatrix} -9.73 & -1.74 & -0.469 & -0.0896 \\ -1.89 & -3.76 & -0.0968 & -0.162 \end{bmatrix},$$
$$H_{12} = 10^3 \times \begin{bmatrix} 0.312 & 0.159 \\ 0.152 & 0.0302 \end{bmatrix},$$
$$L_{11} = \begin{bmatrix} 14.7 & -1.13 & 0.47 & -0.04 & 0.004 & -3 \times 10^{-4} \\ -6.37 & 15.2 & -0.21 & 0.49 & -0.002 & 3.9 \times 10^{-4} \end{bmatrix},$$
$$L_{12} = \begin{bmatrix} 12.3 & 0.634 & 0.395 & 0.0205 & 0.0032 & 0.0002 \\ 3.82 & 11.8 & 0.123 & 0.380 & 0.0010 & 0.0031 \end{bmatrix},$$

with $\alpha = 20$ and $Q = \text{diag}(10^{-5}, 10^{-5}, 1, 1)$. For conciseness, the details on the 32-rules PDC controller obtained from Theorem 1 with the same values of α and Q are omitted. From Remark 4, the computation of the controller gains via a robust compensation scheme can be significantly simplified, see Table 2.

Table 2 Computation Costs.

Number of rules	32-rules	16-rules	8-rules	4-rules
$\mathcal{N}_{var}$	5138	1298	338	98
$\mathcal{N}_{row}$	33816	8728	2328	664

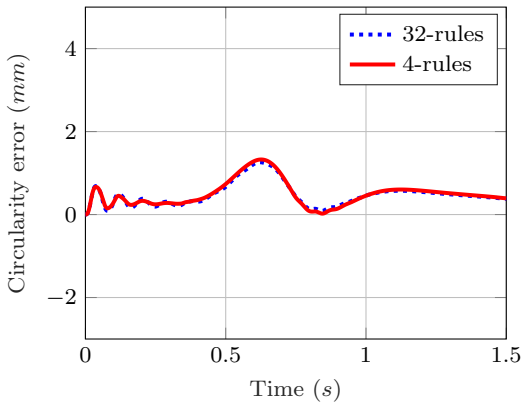

Fig. 4 Circularity errors in Case 1 obtained with 32-rules controller (dotted blue), with 4-rules controller (solid red).

The reference trajectory in the $x - y$ plane as well as those obtained for the robot effector are depicted in Fig. 2 for the nominal case. As shown on this figure, the obtained performance are similar for the two controllers. This can be confirmed by the circularity errors shown in Fig. 4) for which the maximal deviation with

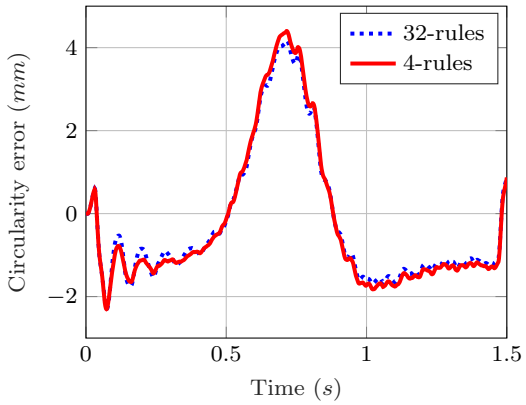

Fig. 5 Circularity errors in Case 2 obtained with 32-rules controller (dotted blue), with 4-rules controller (solid red).

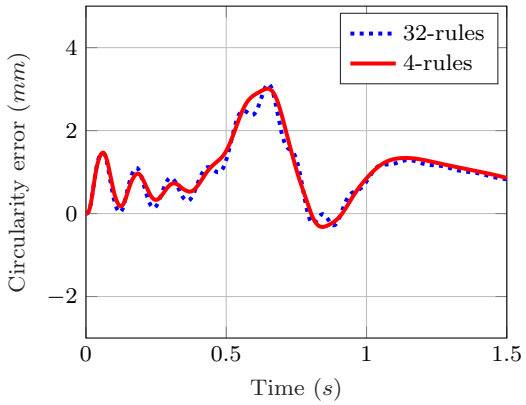

Fig. 6 Circularity errors in Case 3 obtained with 32-rules controller (dotted blue), with 4-rules controller (solid red).

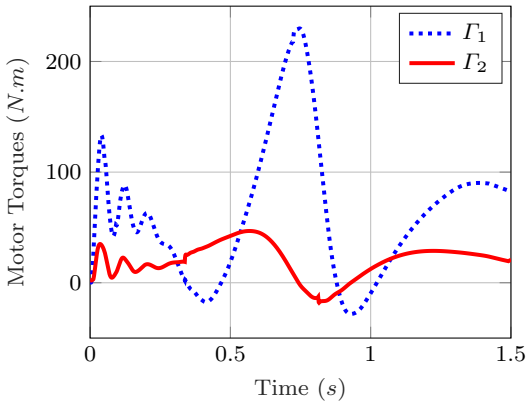

Fig. 7 Actuator torques in Case 1: actuator 1 (dotted blue), actuator 2 (solid red).

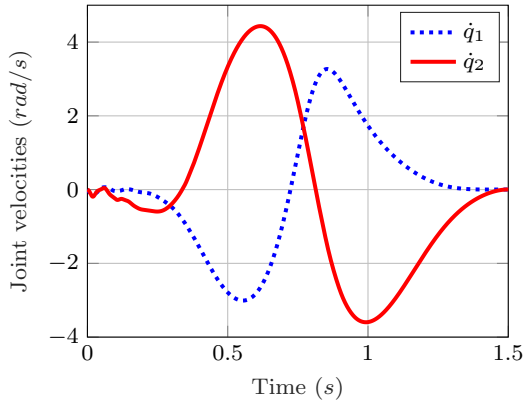

Fig. 8 Joint velocities in the nominal case: joint 1 (dotted blue), joint 2 (solid red).

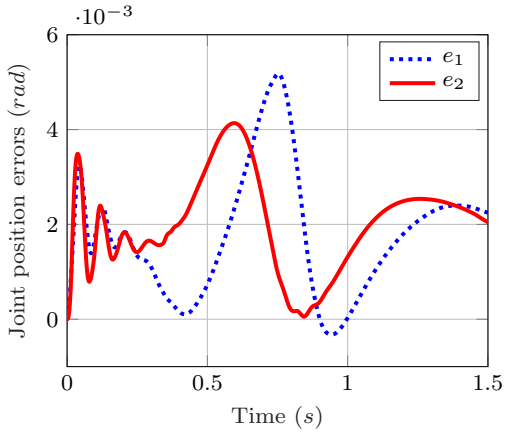

Fig. 9 Joint position errors in the nominal case: joint 1 (dotted blue), joint 2 (dashed blue).

respect to the radius of the reference trajectory is about 1.3 mm for the two controllers. The circularity errors are also plotted in the two operating conditions (Cases 2 and 3) in Figs. 5 & 6. Here again the behaviour obtained for the two controllers are similar, the worst one being with respect to the external force applied (Case 2) for which the trajectory radius evolutes between −2.3 and 4.4 mm. Both cases show the robustness of the tracking performance to external disturbances (machining force) and uncertainties (load variation). The actuator torques are given in Fig. 7 for the 4-rules controller in the nominal case. The maximal required torques are 228 Nm for joint 1 and 47 Nm for joint 2. Joint velocities are shown in Fig. 8, and the friction forces applied on the two joints in Fig. 10. The tracking errors of angular positions are shown in Fig. 9 confirming the good tracking performance obtained using the proposed approach.

7 Concluding Remarks

A robust T-S fuzzy descriptor approach was applied to control a nonlinear 2-DoF serial manipulator. This approach can not only guarantee a high $\mathcal{H}_\infty$ tracking performance but also allow the complexity reduction of both control design and implementation of the controllers. Keeping the descriptor form stemmed from the mechanical modeling of robot manipulators while considering only essential nonlinearities for control design,

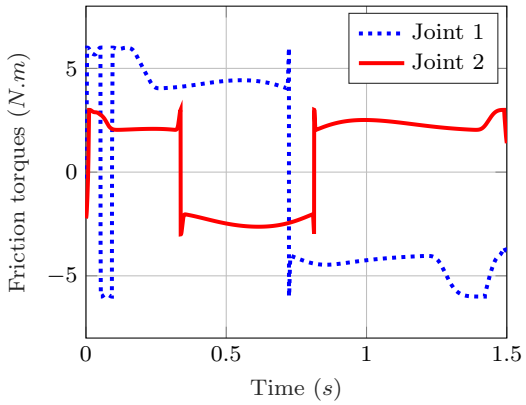

Fig. 10 Friction torques: joint 1 (dotted blue), joint 2 (solid red).

the proposed nonlinear control approach allows dealing with more complex manipulators compared to the standard T-S control methodology. Application to a two DoF serial manipulator have clearly proved the effectiveness of the new approach despite the existence of unmodeled phenomena such as dry frictions, external disturbances, or parametric variations. Future works focus on the design of a robust output feedback scheme requiring only position measurements for real-time control implementation [36].

References

1. X.-G. Lu, M. Liu, and J.-X. Liu, "Design and optimization of interval type-2 fuzzy logic controller for delta parallel robot trajectory control," *Int. J. Fuzzy Syst.*, vol. 19, no. 1, pp. 190–206, 2017.
2. Y. Pan, H. Wang, X. Li, and H. Yu, "Adaptive command-filtered backstepping control of robot arms with compliant actuators," *IEEE Trans. Control Syst. Technol.*, vol. 26, no. 3, pp. 1149–1156, 2018.
3. D. Nojavanzadeh and M. Badamchizadeh, "Adaptive fractional-order non-singular fast terminal sliding mode control for robot manipulators," *IET Control Theory Appl.*, vol. 10, no. 13, pp. 1565–1572, 2016.
4. C.-C. Tsai, M.-B. Cheng, and S.-C. Lin, "Robust tracking control for a wheeled mobile manipulator with dual arms using hybrid sliding-mode neural network," *Asian J. Control*, vol. 9, no. 4, pp. 377–389, 2007.
5. H.-C. Huang and C.-H. Chiang, "Backstepping holonomic tracking control of wheeled robots using an evolutionary fuzzy system with qualified ant colony optimization," *Int. J. Fuzzy Syst.*, vol. 18, no. 1, pp. 28–40, 2016.
6. P. Ouyang, J. Acob, and V. Pano, "PD with sliding mode control for trajectory tracking of robotic system," *Robot. Comput. Integr. Manuf.*, vol. 30, no. 2, pp. 189–200, 2014.
7. E. Hedberg, M. Norrlöf, S. Moberg, and S. Gunnarsson, "Comparing feedback linearization and Jacobian linearization for LQ control of an industrial manipulator," in *Proc. 12th IFAC Symp. Robot Control*, 2018.
8. Y. Pi and X. Wang, "Trajectory tracking control of a 6-DOF hydraulic parallel robot manipulator with uncertain load disturbances," *Control Eng. Pract.*, vol. 19, no. 2, pp. 185–193, 2011.
9. E. M. Jafarov, M. A. Parlakci, and Y. Istefanopulos, "A new variable structure PID-controller design for robot manipulators," *IEEE Trans. Control Syst. Technol.*, vol. 13, no. 1, pp. 122–130, 2005.
10. S. Purwar, I. N. Kar, and A. N. Jha, "Adaptive output feedback tracking control of robot manipulators using position measurements only," *Expert Syst. Appl.*, vol. 34, no. 4, pp. 2789–2798, 2008.
11. Q. Hu, L. Xu, and A. Zhang, "Adaptive backstepping trajectory tracking control of robot manipulator," *J. Franklin Inst.*, vol. 349, no. 3, pp. 1087–1105, 2012.
12. Y. Pan and H. Yu, "Composite learning robot control with guaranteed parameter convergence," *Automatica*, vol. 89, pp. 398–406, 2018.
13. C.-S. Tseng, B.-S. Chen, and H.-J. Uang, "Fuzzy tracking control design for nonlinear dynamic systems via T-S fuzzy model," *IEEE Trans. Fuzzy Syst.*, vol. 9, no. 3, pp. 381–392, 2001.
14. A.-T. Nguyen, M. Dambrine, and J. Lauber, "Lyapunov-based robust control design for a class of switching nonlinear systems subject to input saturation: application to engine control," *IET Control Theory Appl.*, vol. 8, pp. 1789–1802, 2014.
15. L. Vermeiren, A. Dequidt, M. Afroun, and T.-M. Guerra, "Motion control of planar parallel robot using the fuzzy descriptor system approach," *ISA Trans.*, vol. 51, no. 5, pp. 596–608, 2012.
16. T. Takagi and M. Sugeno, "Fuzzy identification of systems and its applications to modeling and control," *IEEE Trans. Syst. Man, Cybern. B, Cybern.*, vol. SMC-15, no. 1, pp. 116–132, 1985.
17. K. Tanaka and H. O. Wang, *Fuzzy Control Systems Design and Analysis: A Linear Matrix Inequality Approach*. John Wiley & Sons, 2004.
18. H. Zhang and D. Liu, *Fuzzy Modeling and Fuzzy Control*. Birkhauser, 2006.
19. J. H. Lilly, *Fuzzy Control and Identification*. John Wiley & Sons, Inc., 2010.
20. Z. Lendek, T. M. Guerra, R. Babuška, and B. De Schutter, *Stability Analysis and Nonlinear Observer Design Using Takagi-Sugeno Fuzzy Models*. Springer, Berlin, Heidelberg, 2011, vol. 262.
21. A.-T. Nguyen, T. Taniguchi, L. Eciolaza, V. Campos, R. Palhares, and M. Sugeno, "Fuzzy control systems: Past, present and future," *IEEE Comput. Intell. Mag.*, vol. 14, no. 1, pp. 56–68, Feb. 2019.
22. A.-T. Nguyen, C. Sentouh, and J.-C. Popieul, "Driver-automation cooperative approach for shared steering control under multiple system constraints: Design and experiments," *IEEE Trans. Ind. Electron.*, vol. 64, no. 5, pp. 3819–3830, 2017.
23. B.-S. Chen and C.-H. Wu, "Robust optimal reference-tracking design method for stochastic synthetic biology systems: T–S fuzzy approach," *IEEE Trans. Fuzzy Syst.*, vol. 18, no. 6, pp. 1144–1159, 2010.
24. X. Hu, L. Wu, C. Hu, and H. Gao, "Fuzzy guaranteed cost tracking control for a flexible air-breathing hypersonic vehicle," *IET Control Theory Appl.*, vol. 6, no. 9, pp. 1238–1249, 2012.
25. C.-Y. Hung, P. Liu, and K.-Y. Lian, "Fuzzy virtual reference model sensorless tracking control for linear induction motors," *IEEE Trans. Cybern.*, vol. 43, no. 3, pp. 970–981, 2013.
26. T. Taniguchi, K. Tanaka, and H. O. Wang, "Fuzzy descriptor systems and nonlinear model following control," *IEEE Trans. Fuzzy Syst.*, vol. 8, no. 4, pp. 442–452, 2000.

27. M. W. Spong, "Modeling and control of elastic joint robots," *J. Dyn. Syst. Meas. Control*, vol. 109, no. 4, pp. 310–318, 1987.
28. S. Andersson, A. Söderberg, and S. Björklund, "Friction models for sliding dry, boundary and mixed lubricated contacts," *Tribol. Int.*, vol. 40, no. 4, pp. 580–587, 2007.
29. M. Makarov, M. Grossard, P. Rodríguez-Ayerbe, and D. Dumur, "Modeling and preview H_∞ control design for motion control of elastic-joint robots with uncertainties," *IEEE Trans. Ind. Electron.*, vol. 63, no. 10, pp. 6429–6438, 2016.
30. A. J. van der Schaft, "$\mathcal{L}_2-$gain analysis of nonlinear systems and nonlinear state-feedback $\mathcal{H}_\infty$ control," *IEEE Trans. Autom. Control*, vol. 37, no. 6, pp. 770–784, 1992.
31. T. M. Guerra, M. Bernal, K. Guelton, and S. Labiod, "Non-quadratic local stabilization for continuous-time Takagi-Sugeno models," *Fuzzy Sets Syst.*, vol. 201, pp. 40–54, 2012.
32. A.-T. Nguyen, R. Márquez, T.-M. Guerra, and A. Dequidt, "Improved lmi conditions for local quadratic stabilization of constrained Takagi-Sugeno fuzzy systems," *Int. J. Fuzzy Syst.*, vol. 19, no. 1, pp. 225–237, 2017.
33. A.-T. Nguyen, R. Márquez, and A. Dequidt, "An augmented system approach for LMI-based control design of constrained Takagi-Sugeno fuzzy systems," *Eng. Appl. Artif. Intell.*, vol. 61, pp. 96–102, 2017.
34. J. Löfberg, "YALMIP: A toolbox for modeling and optimization in MATLAB," in *IEEE Int. Symp. Comput. Aided Control Syst. Des.*, Taipei, 2004, pp. 284–289.
35. K. Toh, M. Todd, and R. Tutuncu, "SDPT3 — a Matlab software package for semidefinite programming, version 1.3," *Optimization Methods and Software*, vol. 11, pp. 545–581, 1999.
36. A.-T. Nguyen, C. Sentouh, and J. Popieul, "Sensor reduction for driver-automation shared steering control via an adaptive authority allocation strategy," *IEEE/ASME Trans. Mechatron.*, vol. 23, no. 1, pp. 5–16, 2018.